Available online at www.sciencedirect.com

SciVerse ScienceDirect

Ceramics International 39 (2013) 1645–1650

CERAMICS INTERNATIONAL

www.elsevier.com/locate/ceramint

Structural, magnetic and electronic structure properties of pure and Ti doped $Mg_{0.95}Mn_{0.05}Fe_2O_4$ nanocrystalline thin films

Shalendra Kumar[a,*], Faheem Ahmed[b], M.S. Anwar[b], B.H. Koo[b], H.K. Choi[b], S. Gautam[c], K.H. Chae[c], Hanshik Chung[d]

[a]*Department of Physics, Pohang University of Science and Technology, Pohang 790–784, Republic of Korea*
[b]*School of Nano and Advanced Materials Engineering, Changwon National University, 9 Sarim dong, Changwon-641-773, Republic of Korea*
[c]*Advanced Analysis Center, Korea Institute of Science and Technology, Seoul 136-791, Republic of Korea*
[d]*Department of Mechanical and Precision Engineering and The Institute of Marine Industry, Gyeongsang National University, Tongyeong 650-160, Republic of Korea*

Received 7 June 2012; received in revised form 23 July 2012; accepted 31 July 2012
Available online 11 August 2012

Abstract

Thin films of pure and Ti doped $Mg_{0.95}Mn_{0.05}Fe_2O_4$ deposited using pulsed laser deposition technique, have been characterized using X-ray diffraction, Raman spectroscopy, dc magnetization, atomic force microscopy, magnetic force microscopy and near edge X-ray absorption fine structure spectroscopy measurements. X-ray diffraction and Raman spectroscopy measurements indicate that both the films have single phase and the polycrystalline behavior with FCC structure. The grain size calculated using XRD data was 18 and 27 nm for pure and Ti doped films, respectively. Magnetic measurements reflect that pure film has superparamagnetic behavior while Ti doped film has soft ferrimagnetic behavior at room temperature. Atomic force microscopy measurements indicate that both the films are nanocrystalline in nature. Near edge X-ray absorption fine structure spectroscopy measurements clearly infer that Fe ions are in mixed valence state.

Keywords: Spinel ferrite; Raman spectroscopy; XRD; PLD

1. Introduction

During the last decades, there has been a considerable interest in the study of ferrite materials due to their large interest in various potential applications as well as to understand the undergoing physical processes to tailor these materials for modern technology [1–6]. Ferrite films are of particular interest for high frequency applications because of their low conductivity, and thus lower eddy current losses as compared to metal alloy films, and their high saturation magnetizations and Curie temperatures as compared to garnet films. Many groups have used a variety of thin film growth techniques, including pulsed laser deposition (PLD), sputtering, and electron beam reactive evaporation to synthesize the spinel ferrites [7–9]. However, PLD shows some advantages especially for growing the multi-component materials in both final stoichiometry and the low substrate temperature needed to obtain the crystallinity [10,11]. Ferrite thin films deposited using PLD have been found to have the excellent magnetic properties in good agreement with the bulk system. Among the family of spinel ferrites, Mg–Mn ferrite has unique physical properties such as: rectangular hysteresis loop, high resistivity and low eddy current loss, which make it suitable for the technological application such as: memory devices, switching circuit in the digital computers and humidity sensors [12–14]. In the present work, we have studied the structural, magnetic and electronic structure properties of pure and 10% Ti doped $Mg_{0.95}Mn_{0.05}Fe_2O_4$ thin films using X-ray diffraction, Raman spectroscopy, dc magnetization, magnetic force microscopy and near edge X-ray absorption fine structure spectroscopy measurements. The surface morphology of

*Corresponding author.
E-mail address: shailuphy@gmail.com (S. Kumar).

0272-8842/$ - see front matter © 2012 Elsevier Ltd and Techna Group S.r.l. All rights reserved.
http://dx.doi.org/10.1016/j.ceramint.2012.07.113

the films was studied using atomic force microscopy measurements.

2. Experimental

Polycrystalline bulk targets of pure and 10% Ti doped $Mg_{0.95}Mn_{0.05}Fe_2O_4$ were prepared by conventional solid-state reaction method. The stoichiometric amounts of high purity metal oxides MgO, FeO, TiO_2 and MnO_2 were mixed thoroughly and pre-calcinated at 1000 °C for 12 h. The pre-calcinated materials were again ground and calcinated at 1250 °C for 24 h. Finally, the samples were ground to fine powder, pressed into pellet form and sintered at 1300 °C for 24 h and used for the deposition of thin films. The KrF excimer laser (Lambda Physik model COMPEX-201) of wavelength 248 nm and pulse duration of 20 ns was used to deposit the thin films from a 25 mm diameter polycrystalline pure and 10% Ti doped $Mg_{0.95}Mn_{0.05}Fe_2O_4$ target on to 1 cm × 1 cm Pt–Si substrate. The energy density of the laser pulse was kept at 2 J/cm^2 and repetition rate at 10 Hz. Substrate heating was provided by attaching the Pt–Si substrate using silver paste to a radiatively heated stainless steel block which was positioned 5 cm from the target. The substrate temperature was maintained at 400 °C during the deposition to get good adhesion. Before the deposition, the chamber was evacuated to 10^{-6} Torr vacuum and then the pressure was increased to 300 m Torr of oxygen during the deposition. The focused laser beam was incident on the target surface at an angle of 45°. The target was rotated at about 10 rpm. After deposition, the thin films were cooled slowly to room temperature at the rate of 5°C/min. maintaining the oxygen pressure in the vacuum chamber to 300 mTorr. The film thickness was about 300 nm as measured by Talystep profilometer (Ambios Inc. USA) with 0.5 nm resolution. X-ray diffraction (XRD) measurements were performed for phase identification and orientation of the thin films using Bruker AXE D8 X-ray diffractometer with CuK_α radiation at room temperature. Micro-Raman and dc magnetization measurements were performed by a Renishaw Raman spectrometer working with an excitation wavelength of 514 nm from Ar ion laser and Quantum Design physical properties measurement setup (Model-6000), respectively. The magnetization versus field loops were measured at room temperature by applying the maximum field of 2 kOe. Surface morphology and magnetic structures measurements were performed using atomic force microscopy (AFM) and magnetic force microscopy (Digital Nano-Scope III). The local environment and valence state of iron within the films were determined by using NEXAFS. The NEXAFS measurement of undoped and Ti doped $Mg_{0.95}Mn_{0.05}Fe_2O_4$ along with the reference compounds of Fe_2O_3, Fe_3O_4, and FeO, at Fe $L_{3,2}$ –edges were performed at the soft X-ray beam line 10D XAS KIST of the Pohang Accelerator Laboratory (PAL), operating at 3 GeV with a maximum storage current of 200 mA. The spectra were simultaneously collected in the total electron yield (TEY) mode and the fluorescence yield (FY) mode at room temperature in a vacuum better than 1.5×10^{-8} Torr. The spectra in the two modes turned out to be nearly identical indicating that the systems are so stable that the surface contamination effects are negligible even in the TEY mode. The spectra were normalized to incident photon flux and the energy resolution was better than 0.2 eV. The obtained NEXAFS spectra were normalized and processed using Athena 0.8.056.

3. Results and discussion

Fig. 1 highlights the XRD patterns of pure and 10% Ti doped $Mg_{0.95}Mn_{0.05}Fe_2O_4$ films deposited on Pt–Si substrate. It is clear from the XRD pattern that both the films exhibit single phase polycrystalline behavior with face centered cubic (FCC) structure. It is observed that the intensity of the diffraction peaks increases in case of Ti doped sample which indicates that the doped film has good crystallinity as compared to undoped film. By having a closure look on the XRD spectra, it is found that peaks position shifted towards the the higher 2θ value for the Ti doped film, which indicates that the lattice parameter decreases with the Ti doping. The average size of the grain was estimated from the broadening of X-ray diffraction peak using Scherrer's equation [15]

$$d = \frac{0.89\lambda}{\beta \cos\theta_B}$$

where $\beta = (\beta_M^2 - \beta_i^2)^{1/2}$. Here λ is X-ray wavelength (1.54 Å for CuK_α), β_M and β_i is the measured and instrumental broadening in radians respectively and θ_B is Bragg's angle in degrees. The calculated value of the average grain size for the pure and Ti doped film was found 18 ± 2 and 27 ± 2 nm, respectively, which indicate that both the films are composed of nano-crystallites.

Fig. 2 shows the Raman spectra of pure and 10% Ti doped $Mg_{0.95}Mn_{0.05}Fe_2O_4$ films measured at room temperature.

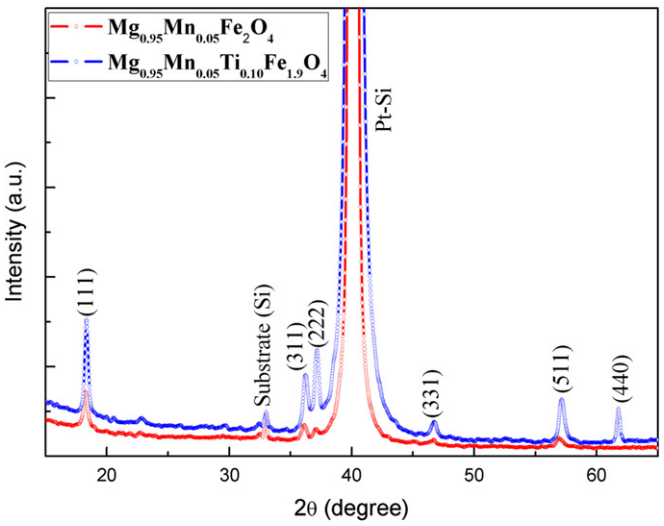

Fig. 1. XRD pattern of pure and 10% Ti doped $Mg_{0.95}Mn_{0.05}Fe_2O_4$ thin films.

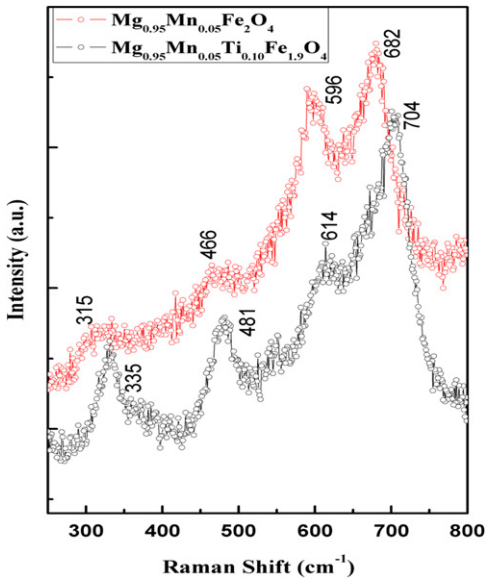

Fig. 2. Raman spectra of pure and 10% Ti doped $Mg_{0.95}Mn_{0.05}Fe_2O_4$ thin films.

Spinel ferrite has the mixed cubic spinel structure belonging to the space group $O_h^7(Fd\bar{3}m)$ [16]. The unit cell of the spinel ferrite consists of eight formulae unit ($Z=8$), the smallest Bravais cell contains only 14 atoms ($Z=2$). The Mg and Fe atoms occupy both the tetrahedral (8*a*) and octahedral (16*d*) sites. The oxygen atoms are in (32*e*) site symmetry positions. The factor group analysis predicts the following possible modes in the spinel system [17]:

$$A_{1g}(R)+E_g(R)+F_{1g}+3F_{2g}(R)+2A_{2u}+2E_u+4F_{1u}(IR)+2F_{2u}$$

According to the analysis (after subtracting the acoustic and silent modes) one can expect 5 Raman and 4 infrared active modes. Experimentally in the present system, we have observed only four Raman active modes at room temperature (See Fig. 2). In case of the undoped film, the Raman modes are observed at 315, 466, 596 and 682 cm^{-1}, respectively. However, in case of Ti doped film, these modes were observed at 335, 481, 614 and 704 cm^{-1}, respectively. The peaks at 596/614 cm^{-1} and 682/704 cm^{-1} are attributed to the T-site mode that reflects the local lattice effect in the tetrahedral sub-lattice whereas the other peaks at 315/335 cm^{-1} and 466/481 cm^{-1} correspond to the O-site mode and reflects the local lattice effects in the octahedral sub-lattice. It can be seen from the Raman spectra that the Ti doped film has the Raman shift as compared to the pure film. Moreover, it is observed that the intensity of the Raman modes increases in case of Ti doped film.

Atomic force microscopy (AFM) measurements were carried out to study the morphology of the thin films. Fig. 3(a) and (b) represents the 2-dimensional (right panel) and 3-dimensional (left panel) view of the surface morphology of the pure and Ti doped films. It can be clearly seen from the morphology that both the films are composed of nanocrystalline grains which are in good agreement with XRD results. The computed values of the average roughness for pure and Ti doped films were found 0.421 and 1.6 nm, respectively. A computed value of the average roughness represents the root-mean-square variation (i.e. standard deviation) of the surface height profile from the mean height, (R_{rms}) and is defined as

$$R_{rms}=\left[\frac{1}{N}\sum_{i=1}^{N}(y_i-\overline{y})^2\right]^{1/2}$$

where N is number of data points of the profile, y_i are the data points that describes the relative vertical height of the surface, and $\overline{y}$ is the mean height of the surface. A closure look on the AFM micrograph indicates that the crystallite size of pure film is smaller than doped film. Fig. 4(a) and (b) shows the magnetic force microscopy (MFM) measurements performed at a lift at 20 nm for pure and Ti doped films. From the analysis of MFM data, we have calculated the corresponding root mean square (RMS) phase shifts. The phase shift values for pure and doped films are 0.28 and 0.99 nm, respectively. The increased value of phase shift undoubtedly indicates that Ti doped film has good magnetic signal. In order to determine the magnetic behavior, we have done the *M–H* hysteresis loop measurements at 300 K for pure and Ti doped films as shown in Fig. 5. The hysteresis curves demonstrate that pure film exhibits a superparamagnetic behavior and the curve passes through the origin ($H=0$) whereas Ti doped film shows the ferrimagnetic ordering at room temperature. The M_S value for Ti doped film, obtained by plotting magnetization versus $1/H$ curve and extrapolating the $1/H\rightarrow 0$, is 45 emu/cm^3, which is less than that of the bulk sample [18]. The value of H_C and remanance (M_r) for the Ti doped film has been found to be larger than that of bulk sample. The higher value of H_C may be due to the formation of defects in the form of grain boundary and point defects, etc. during the growth of the thin film which acts as pinning sites for domain walls. The another reason may be due to the size effects [19], which is smaller in case of thin films as compared to the bulk sample. According to Kittel's theory [20,21], grain size (or particle) is inversely proportional to H_C. This means that the decrease in the particle size results increase in the value of coercivity. However, it is observed that below a critical diameter of the particle (say D), which is not well-defined, the particle become single domain and in this size range the coercivity has maximum value. When the particle size decreases below the D, the coercivity start decreasing according to the relation [22], $H_c=g-h/D^{3/2}$, where g and h are constants. Below a certain diameter (D), the coercivity becomes almost zero due to the thermal effects, which are strong enough to spontaneously demagnetize a previously saturated assembly of particles. In contrary, pure film does not show any hysteresis loop at room temperature and curve passes through origin ($H=0$), which reflects its superparamagnetic behavior at room temperature. This can be attributed to the smaller grain size (18 nm).

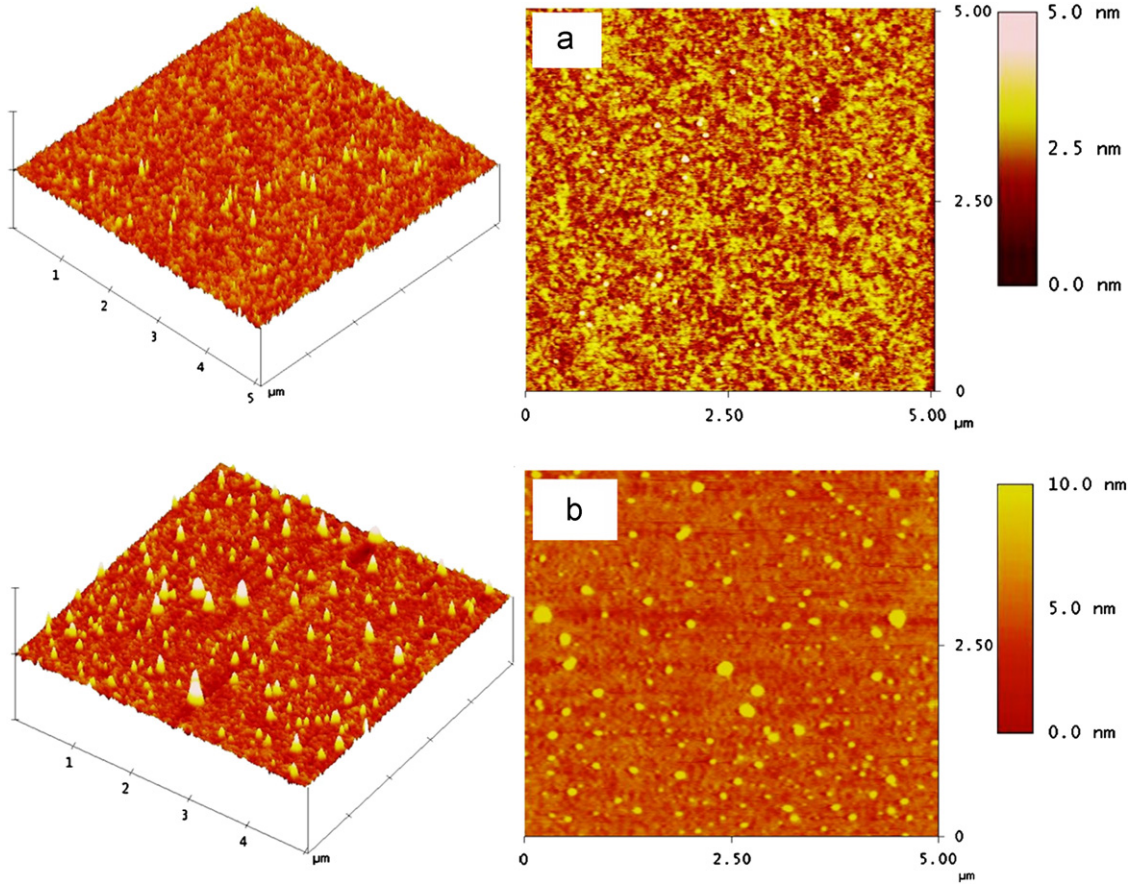

Fig. 3. Two and three dimensional view of atomic force microscopy (AFM) micrographs for (a) $Mg_{0.95}Mn_{0.05}Fe_2O_4$ film, and (b) 10% Ti doped $Mg_{0.95}Mn_{0.05}Fe_2O_4$ thin films.

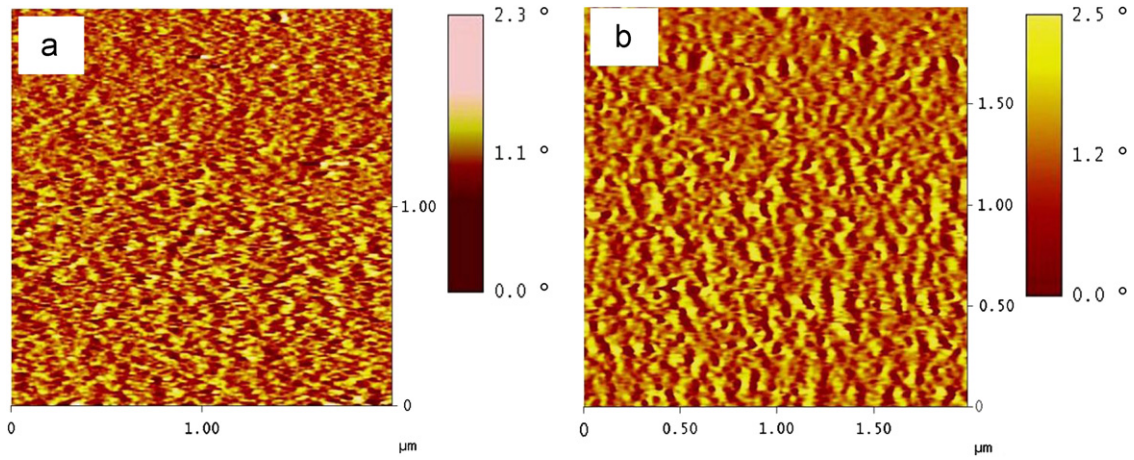

Fig. 4. Magnetic force microscopy (MFM) images taken at a lift height of 20 nm for (a) $Mg_{0.95}Mn_{0.05}Fe_2O_4$ film, and (b) 10% Ti doped $Mg_{0.95}Mn_{0.05}Fe_2O_4$ thin film.

In order to know about the effect of Ti doping on the valence state of Fe ion, we have performed Fe $L_{3,2}$ NEXAFS measurements. In general, the $L_{3,2}$ edge of $3d$ transitions metals (TM) entails information regarding the coordination, the valence state and site symmetry of the TM. The $L_{3,2}$ edge involves the electrical dipole allowed $2p \rightarrow 3d$ transitions. The L_3 edge originates from the electron transition from the inner $2p_{3/2}$ orbitals to empty $3d$ orbitals of the metal and L_2 edge originates from $2p_{1/2}$–$3d$ electron transitions [23]. The splitting of the Fe $L_3(2p_{3/2})$ and $L_2(2p_{1/2})$ multiplet structures are separated by a $2p$ spin orbital splitting of $\sim$12.3 eV and the intensity of the L edge is directly proportional to the Fe

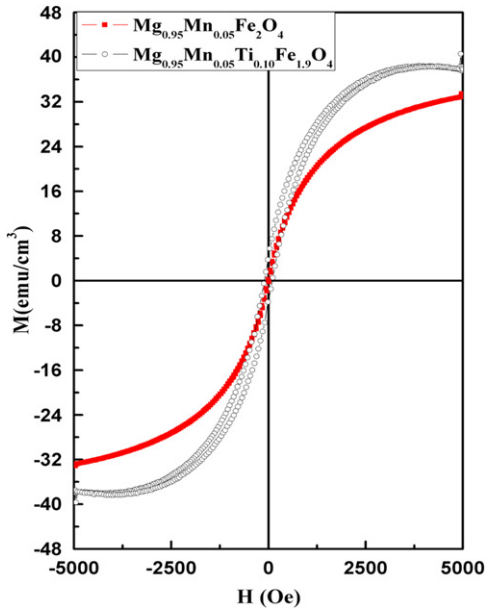

Fig. 5. M–H hysteresis curve at 300 K for pure and 10% Ti doped $Mg_{0.95}Mn_{0.05}Fe_2O_4$ thin films.

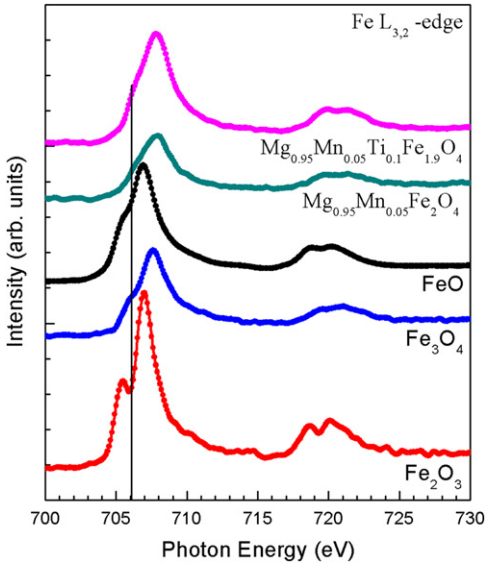

Fig. 6. (Color online) Normalized Fe $L_{3,2}$-edge spectra of pure and 10% Ti doped $Mg_{0.95}Mn_{0.05}Fe_2O_4$ thin films plotted with reference spectra FeO(Fe^{2+}), Fe^2O^3(Fe^{3+}) and Fe^3O^4(Fe^{2+}/Fe^{3+}) for comparison.

d character in the unoccupied and partially occupied valence orbital of the metals. The spectral shape of the TM ions are very sensitive to both the ligand field and *d*-orbital covalency. Fig. 6 represents the normalized Fe $L_{3,2}$-edge NEXAFS spectra of pure and 10% Ti doped $Mg_{0.95}Mn_{0.05}Fe_2O_4$ thin films along with the reference compounds Fe_3O_4, Fe_2O_3 and FeO. It can be seen from the spectral features of the reference compounds that the main difference is at the L_3 edge which is due to the diversity of electron configuration in 3*d* orbitals of Fe ions (Fe^{2+} or Fe^{3+}) and coordination as well as because of the site symmetry of the Fe atom (tetrahedral or octahedral). The L_3 edge of Fe_2O_3 compound is described by a well-developed doublet with a small intensity peak and a main peak, however, in case of FeO compound, the first peak becomes a shoulder of the main peak. It can be seen in Fig. 6 that the spectral features of pure and 10% Ti doped $Mg_{0.95}Mn_{0.05}Fe_2O_4$ thin films particularly at L_3-edge suggest that the spectral features are similar to Fe_3O_4 which infers that Fe is in mixed valence state. Therefore, it is exciting to study the Fe valence state with Ti doping. The NEXAFS spectra can be roughly understood as the superposition of the independent contribution from Fe^{3+} and Fe^{2+} ions under the O_h and T_d local symmetry. Earlier, it was reported that the multiplet structures of Fe^{3+} ions are richer than those of Fe^{2+} ions. It can be seen from the Fe $L_{3,2}$ edge NEXAFS spectra that L_3 region exhibits a distinctive shoulder together with the main peak and the shape and position of the shoulder remains same with the Ti substitution. The only difference, we found that the intensity ratio of main peak to the shoulder peak which increase a little with Ti doping and can be explained as (i) the ground state is a mixture of $3d^5L$ (where L denotes a ligand hole) and $3d^6$, or (ii) the ground state remains essentially $3d^5L$, but the $3d^5$ part may contain more than one symmetry.

4. Conclusions

We have successfully grown the nanocrystalline thin film of pure and 10% Ti doped $Mg_{0.95}Mn_{0.05}Fe_2O_4$ using PLD technique. XRD results show that both pure and Ti doped films have single phase nature with FCC structure having grain size 18 and 27 nm, respectively. Magnetization study infers that pure film exhibits superparamagnetic behavior whereas Ti doped film shows ferrimagnetic ordering at room temperature. Root mean square (RMS) phase shifts calculated from MFM data found to have higher value for Ti doped film. NEXAFS measurements indicate that Fe is in mixed valence state in pure and Ti doped thin films.

Acknowledgments

This work was supported by the National Research Foundation of Korea (NRF) grant funded by the Korea government (MEST) 2012-0009450. This work is also supported by BK21 project corp.

References

[1] S. Kumar, S.K. Sharma, Alimuddin, M. Knobel, R.J. Choudhary, C.G. Lee, B.H. Koo, R. Kumar, Structural and magnetic properties of bulk and thin films of $Mg_{0.95}Mn_{0.05}Fe_2O_4$, Current Applied Physics 9 (2009) 1009.

[2] D.C. Khan, M. Misra, A.R. Das, Structure and magnetization studies of Tisubstituted $Ni_{0.3}Zn_{0.7}Fe_2O_4$, Journal of Applied Physics 53 (1982) 2722.

[3] A.R. Das, V.S. Anathan, D.C. Khan, Lattice parameter variation and magnetization studies on titanium, zirconium, and tinsubstituted nickelzinc ferrites, Journal of Applied Physics 57 (1985) 4189.

[4] R.A. Brand, H. Georges-Gibert, J. Hubsch, I.A. Heller, Ferrimagnetic to spin glass transition in the mixed spinel $Mg_{1+t}Fe_{2-2t}Ti_tO_4$: a

Mossbauer and DC susceptibility study, Journal of Physics F: Metal Physics 15 (1985) 1987.
[5] S.K. Sharma, S. Kumar, M. Alimuddin, R.J. Knobel, D.M. Choudhary, C.G. Phase, R. Lee, Kumar Effect of 200 MeV Ag^{15+} ion irradiation on structural and magnetic properties of $Mg_{0.95}Mn_{0.05}Fe_2O_4$ ferrite thin film, Surface and Coatings Technology 203 (2009) 2707.
[6] S. Kumar, R. Kumar, A. Dogra, V.R. Reddy, A. Banerjee, Alimuddin, Mössbauer and magnetic studies of multiferroic $Mg_{0.95}Mn_{0.05}Fe_{2-2x}Ti_{2x}O_4$ system, Journal of Applied Physics 99 (2006) 08M910.
[7] S.H. Cho, H.J. Kim, Effects of additives on the preferred orientation of Mn–Zn ferrite thin films deposited by ion beam sputtering, Applied Physics Letters 66 (1995) 1282.
[8] S. Venzke, R.B. van Dover, J.M. Philips, E.M. Gyorgy, T. Siegrist, C.H. Chen, D. Werder, R.M. Fleming, R.J. Felder, E. Coleman, O. Opila, Epitaxial growth and magnetic behavior of $NiFe_2O_4$ thin films, Journal of Materials Research 11 (1996) 1187.
[9] R. Kumar, M.W. Khan, J.P. Srivastava, S.K. Arora, R.G.S. Sofin, R.J. Choudhary, I.V. Shevert, Swift heavy ion irradiation-induced modifications in structural, magnetic and electrical transport properties of epitaxial magnetite thin films, Journal of Applied Physics 100 (2006) 033703.
[10] D.B. Chrisey, G.K. Hubler Pulsed, Laser Deposition of Thin Films, Wiley, New York, 1994.
[11] H.S. Newman, D.B. Chrisey, J.S. Horwitz, B.D. Weaver, M.E. Reeves, Microwave devices using $YBa_2Cu_3O_{7-}$ films made by pulsed laser deposition, IEEE Transaction on Magnetics 27 (1991) 2540.
[12] I.J. Hegyi, Ferromagnetic spinels with rectangular hysteresis loop, Journal of Applied Physics 25 (1954) 176.
[13] C. Heck, Magnetic Materials and their Applications, Butterworth and Co. (Publishers) Ltd, London, 1974.
[14] N. Rezlescu, E. Rezlescu, C. Doroftei, P.D. Popa, Study of some Mg-based ferrites as humidity sensors, Journal of Physics: Conference Series 15 (2005) 296.
[15] B.D. Cullity, Elements of X-ray Diffraction, Addision-Wesley, London, 1957, p. 261.
[16] G. Turillii, A. Baooluzi, M. Lutennti, L. Tareti, Influence of the particle size and intrinsic magnetic characteristics on the coercivity of sintered magnets, Journal of Magnetism and magnetic materials 104 (2002) 1143.
[17] Z. Wang, P. Lazor, S.K. Saxena, H. Co'Neill St, High pressure Raman spectroscopy of ferrite $MgFe_2O_4$, Materials Research Bulletin 37 (2002) 1689.
[18] S. Kumar, Alimuddin, R. Kumar, P. Thakur, K.H. Chae, B. Angadi, W.K. Choi, Electrical transport, magnetic, and electronic structure studies of $Mg_{0.95}Mn_{0.05}Fe_{2-2x}Ti_{2x}O_{4\pm}$ $(0 \le x \le 0.5)$ ferrites, Journal of Physics: Condensed Matter 19 (2007) 476210.
[19] A. Lisfi, M. Guyot, R. Krishan, M. Porte, P. Rougier, V. Cagan, Microstructure and magnetic properties of spinel and hexagonal ferrimagnetic films prepared by pulsed laser deposition, Journal of Magnetism and Magnetic Materials 157 (1996) 258.
[20] C. Kittel, Theory of the structure of ferromagnetic domains in films and small particles, Physical Review 70 (1946) 965.
[21] C. Kittel, Domain theory and the dependence of the coercive force of fine ferromagnetic powders on particle size, Physical Review 73 (1948) 810.
[22] B.D. Cullity, Introduction to Magnetic Materials, Addision-Wesley, New York, 1972 p 386.
[23] G. van der Laan, I.W. Kirkman, The 2p absorption spectra of 3d transition metal compounds in tetrahedral and octahedral symmetry, Journal of Physics: Condensed Matter 4 (1992) 4189.